

Electronic Supplementary Information

**Synergistic effect of oxygen vacancy and Ni particles
over ZnWO₄/CdS heterostructure for enhancing
photocatalytic reduction and oxidation activities**

Houfeng Zhang ^a, Shenglong Gan ^a, Dongfang Hou ^{a,b,*}, Xiu-qing Qiao ^a, Ru-An
Chi ^{a,b}, Dong-Sheng Li ^{a,b,*}

^a *College of Materials and Chemical Engineering, Key Laboratory of Inorganic Nonmetallic
Crystalline and Energy Conversion Materials, China Three Gorges University, Yichang, Hubei
443002, P.R. China*

^b *Hubei Three Gorges Laboratory, Yichang, Hubei 443007, P. R. China*

***Corresponding authors**

dfhouok@126.com (D. Hou), lidongsheng1@126.com (D. S. Li)

Materials and Characterizations

All chemicals commercially obtained were used directly. Nickel chloride hexahydrate ($\text{NiCl}_2 \cdot 6\text{H}_2\text{O}$) was obtained from Xiya Chemical Technology (Shandong) Co., Ltd. Sodium tungstate dihydrate ($\text{Na}_2\text{WO}_4 \cdot 2\text{H}_2\text{O}$), Zinc chloride (ZnCl_2 , AR), Thiourea ($\text{CS}(\text{NH}_2)_2$, AR) and Cadmium acetate dihydrate ($\text{Cd}(\text{Ac})_2 \cdot 2\text{H}_2\text{O}$) were provided from Sinopharm Chemical Reagent Co., Ltd.

X-ray diffraction (XRD) of the as-obtained products were carried out on the RigakuUltima IV X-ray diffractometer using Cu-K α ($\lambda=1.5418$ nm) radiation. The accelerating voltage and the applied current were at 40 kV and 40 mA, respectively. Scanning electron microscope (SEM, JEOL JSM 7500F), transmission electron microscope (TEM, Tecnai G2 F20 S TWIN) equipped with an energy dispersive spectrometer (EDS) and high-resolution transmission electron microscopy (HRTEM) images were used to observe or determine the morphology and microstructure. X-ray photoelectron spectroscopy (XPS) measurement was taken with the Escalab 250 Xi multifunctional photoelectron spectrometer produced by Thermo Fisher Scientific. The Brunauer–Emmett–Teller (BET) specific surface was determined by nitrogen adsorption in a Belsorp max physical adsorption instrument (Bayer, Japan). The desorption isotherm was used to analysis the pore size distribution by Barrett-Joyner-Halenda (BJH) method. The UV-2550 ultraviolet-visible spectrophotometer produced by Shimadzu Corporation was used to obtain the light absorption performance (Diffuse reflection spectrum, DRS) of the sample at a wavelength range of 200–800 nm. Photo-luminescence (PL) analysis and Time-resolved photoluminescence (TRPL) was recorded with a LS55 fluorescence spectrometer (Perkin-Elmer, USA). The analysis of free radicals was recorded with the electron spin resonance (ESR, JES FA200 spectrometer, Japan) by mixing the photocatalysts in a 5,5-Dimethyl-1-pyrroline N-oxide (DMPO) solution tank (methanol dispersion for $\text{DMPO} \cdot \text{OOH}/\text{O}_2 \cdot$ and aqueous dispersion for $\text{DMPO} \cdot \text{OH}$). And the generation of vacancies was determined by electron paramagnetic resonance (EPR, Bruker, USA). Electrochemical and photoelectrochemical tests were implemented on the CHI 660E electrochemical system in a standard three-electrode quartz cell with the as-prepared samples as the working electrode, a platinum wire (Pt) as the counter electrode, and Ag/AgCl (saturated KCl) as a reference electrode, respectively.

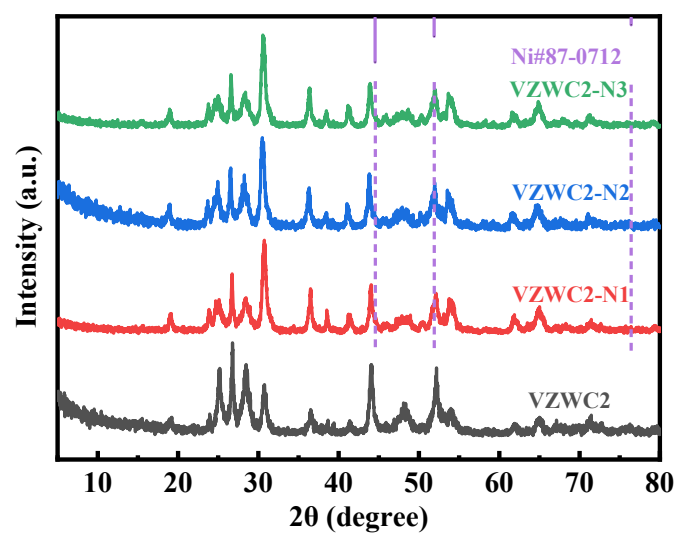


Fig. S1 XRD patterns of VZWC2, VZWC2-N1, VZWC2-N2, and VZWC2-N3

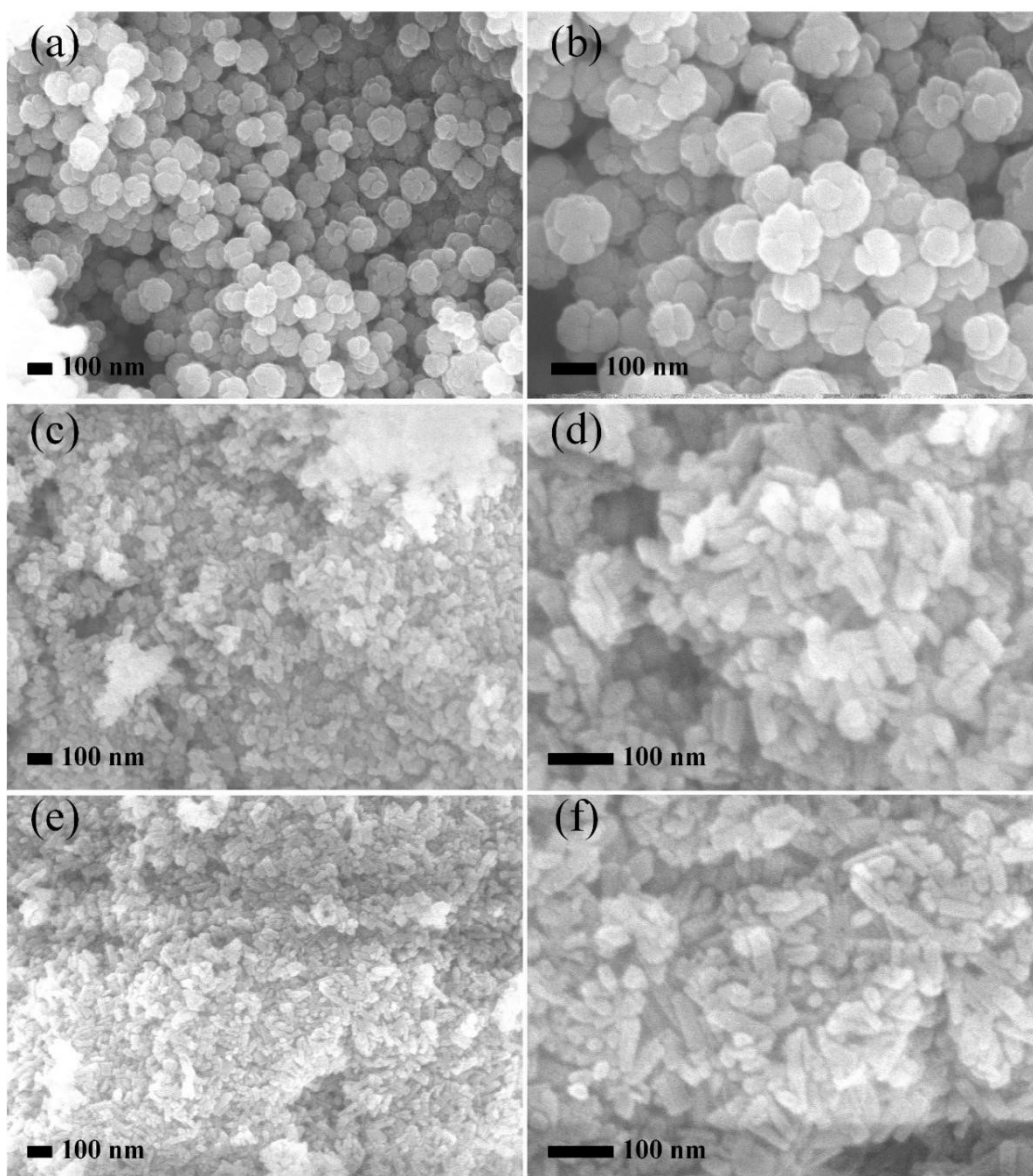


Fig. S2 FESEM images of (a-b) CdS, (c-d) Vo-ZnWO₄,(e-f) ZnWO₄

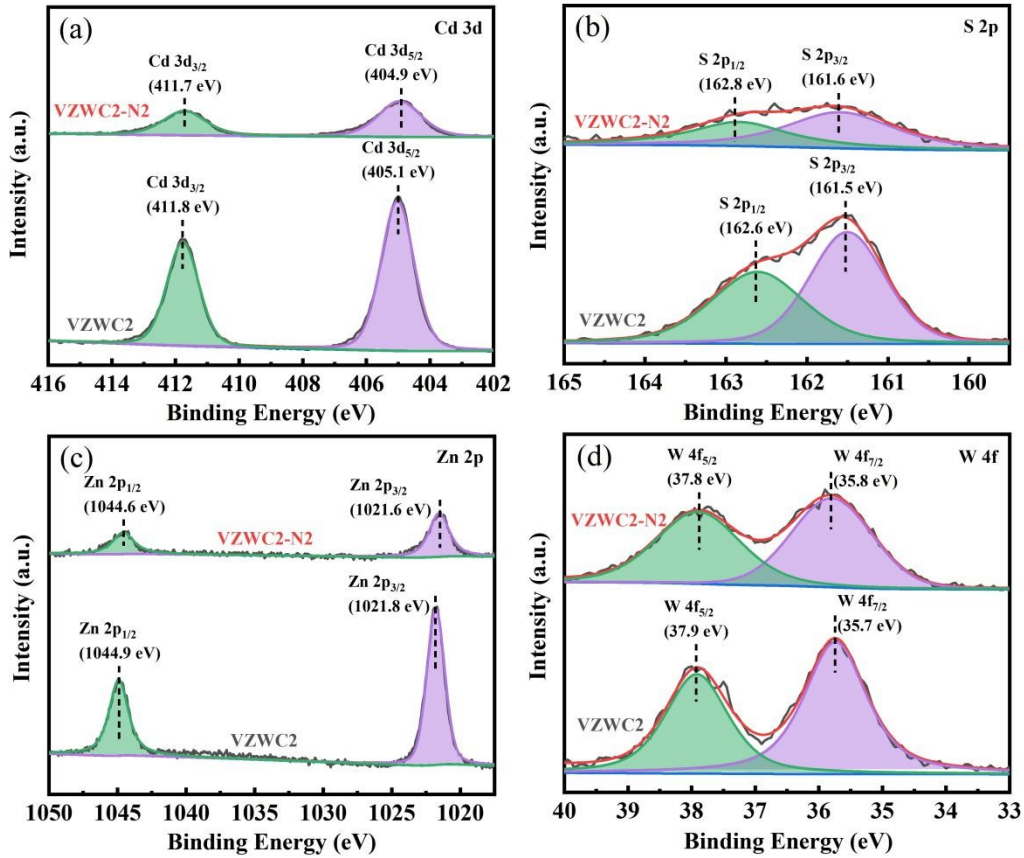


Fig. S3 High-resolution XPS spectra of (a) Cd 3d, (b) S 2p, (c) Zn 2p, (d) W 4f for VZWC2-N2.

Fig. S3a-d shows the XPS spectra of Cd 3d and S 2p, Zn 2p, W4f. In VZWC2, the high-resolution Cd spectrum indicated the existence of Cd 3d 5/2 and 3d 3/2 peaks centered at 411.7 eV and 404.9 eV, respectively. The binding energies of the S 2p 1/2 and 2p 3/2 peaks are located at 162.6 eV and 161.5 eV. The peaks located at 1021.6 eV and 1044.6 eV in the XPS spectrum of Zn 2p could be ascribed to the characteristic peaks of Zn 2p_{3/2} and Zn 2p_{1/2} spin-orbit components of Zn²⁺. The W4f XPS spectra of the V_o-ZnWO₄ surface are simple spin dipoles with BE of 37.8 and 35.8 eV corresponding to W 4f_{5/2} and W 4f_{7/2}, respectively, indicating the presence of the W⁶⁺ state in V_o-ZnWO₄.

Table S1 Summary of material properties

Sample	Specific surface area	Mean pore diameter
Vo-ZnWO ₄	28.820	27.075
CdS	12.696	13.769
VZWC2	22.964	29.039
VZWC2-N2	17.713	35.959

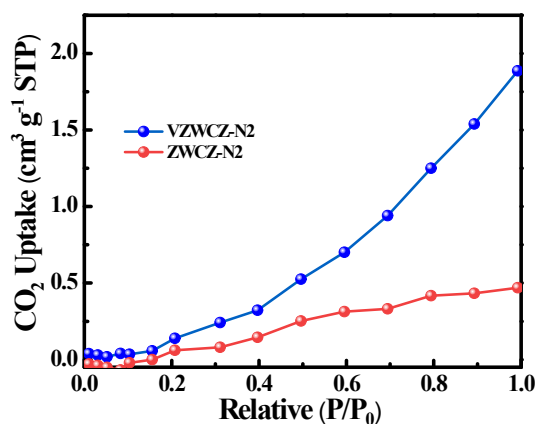


Fig. S4 CO₂ adsorption curves measured at 298 K of VZWC2-N2 and ZWC2-N2.

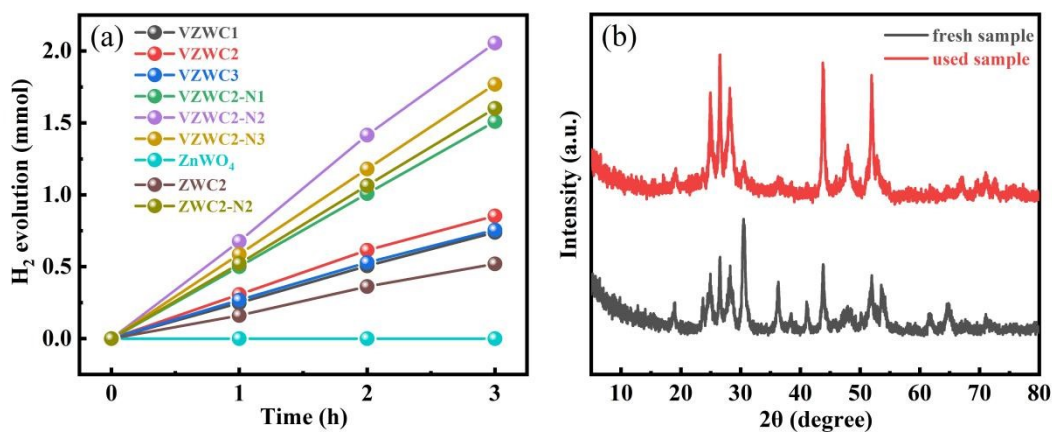


Fig. S5 (a) The comparison of photocatalytic H₂ production activities of different photocatalysts under visible light irradiation. (b) XRD patterns of ZWC2-N2 before and after test.

Table S2 The radiative fluorescence lifetimes and relative percentages of the photoinduced charge carriers in the samples

Sample	τ_1 (ns)	Rel. (%)	τ_2 (ns)	Rel. (%)	τ (ns)
Vo-ZnWO ₄	0.1253	86.24	1.0024	13.76	0.617105
CdS	0.5421	68.21	2.5678	31.79	1.936273
VZWC2	1.9256	48.35	5.2637	8.3649	4.412167
VZWC2-N2	2.1188	58.01	8.3649	41.99	6.745767

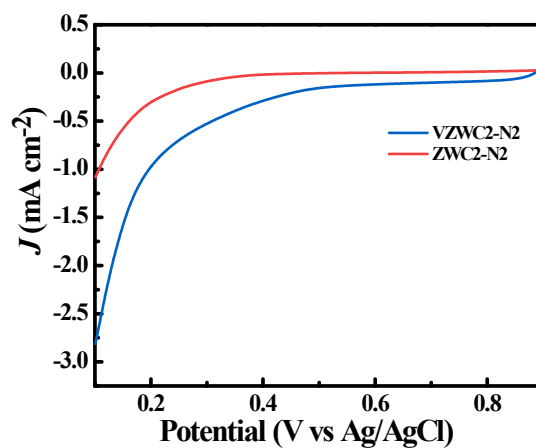


Fig. S6 Linear sweep voltammograms of VZWC2-N2 and ZWC2-N2 in 0.5 M H₂SO₄ aqueous solution.